PDHonline Course C262 (5 PDH)

Rock Blasting Fundamentals

Instructor: Daniel A. Vellone, M.S., P.G.

2020

PDH Online | PDH Center

5272 Meadow Estates Drive
Fairfax, VA 22030-6658
Phone: 703-988-0088
www.PDHonline.com

An Approved Continuing Education Provider

Available online at www.sciencedirect.com
ScienceDirect
International Journal of Rock Mechanics & Mining Sciences 44 (2007) 130–147
International Journal of Rock Mechanics and Mining Sciences
www.elsevier.com/locate/ijrmms

Energy components in rock blasting

José A. Sanchidrián*, Pablo Segarra, Lina M. López

Universidad Politécnica de Madrid, E.T.S.I. Minas. Rios Rosas, 21, 28003 Madrid, Spain

Accepted 18 May 2006
Available online 14 July 2006

Abstract

Ten production blasts and one single-hole confined blast have been monitored in two quarries in order to assess the measurable forms of energy in which the energy delivered by the explosive is transformed in rock blasting. The seismic field from seismographs readings, the initial velocity of the blasted rock face obtained from high-speed video camera records, and the fragment size distributions from image analysis of the muckpile material are used to determine the seismic wave energy, the kinetic energy and the fracture energy, respectively, transferred in the blasting process. The blasting data and the methods of calculation of the energy terms from those are described in detail. Heat of explosion and useful work to 100 MPa have been used as descriptions of the energy of explosives. The maximum total energy measured accounts for not more than 26% of the available explosive energy if this is rated as the heat of explosion, though lower figures are usually obtained. The values measured for each of the energy components range from 2% to 6% of the total energy available for the fragmentation energy, 1–3% for the seismic energy and 3–21% for the kinetic energy. For the confined shothole, the seismic energy was 9% of the heat of explosion. The uncertainty of the calculated energies is analyzed from the variability of the measured data. Particularly important influential parameters are the treatment of the fines tail of the fragment size distribution in the determination of the fragmentation energy, and the use of P or S wave velocity values, and whether these are determined from in situ or from laboratory measurements, in the calculation of the seismic energy.

Keywords: Explosives; Rock blasting; Energy; Fragmentation; Seismic; Rock movement

1. Introduction

Explosives are the primary source of energy for rock breaking in the mining, quarrying and construction industries. The work into which the energy is converted transforms rock into a distribution of fragments and displaces them so that they can be conveniently loaded and hauled for further comminution and processing. Although the energetic qualification of explosives is not particularly high (any fuel/oxygen mixture used in the power industry delivers more energy per unit mass than do explosives), they are compact sources, which are able to deliver their energy in an autonomous form at a very fast rate. This results in reaction products at high pressure that can perform mechanical work in deforming and breaking the material in their vicinity. This is what makes explosives useful and in many cases irreplaceable for rock excavation. This fast energy delivery, in the form of a large amount of reaction products at high pressure and high temperature, is inseparable of a number of transformations other than the desired fragmentation and throw, such as the seismic wave into the rock.

Any explosive data sheet or commercial brochure quotes some type of energetic description. Explosives energy is rated in a variety of ways, obtained either from calculation or from experimental tests. However, the questions of what amount of that explosive energy is transferred to the rock and what fraction of it is converted into efficient work in the usual civil application of rock blasting remains largely undefined. Although the measurement of some of the effects of the explosive in rock is customary (vibration, fragmentation and, to a minor extent, rock movement), they are usually conducted for blast control purpose and the results are rarely cast in terms of their energy content. The reason for this may be that it is not the energy consumption in this or that phenomenon that matters, but rather the end effects, i.e., degree of fragmentation, throw

*Corresponding author. Tel.: +34 913 367 060; fax: +34 913 366 948.
E-mail address: ja.sanchidrian@upm.es (J.A. Sanchidrián).

1365-1609/$ - see front matter © 2006 Elsevier Ltd. All rights reserved.
doi:10.1016/j.ijrmms.2006.05.002

and vibration levels. Data and estimations on energy components in rock blasting are thus limited to a few researchers. Berta [1], Spathis [2] and Ouchterlony et al. [3] calculate the amounts of energy transformed in kinetic energy of the rock, fracture generation and seismic wave. Seismic energy has received special attention since earlier times; calculations of seismic energy and its comparison with explosive energy have been reported by Howell and Budenstein [4], Fogelson et al. [5], Berg and Cook [6], Nicholls [7], Atchinson [8], and more recently by Hinzen [9].

Berta [1] attempted to use some of the energy concepts in his principles of blast design, though this is seldom used in practice. Spathis [2] suggested, as a recommendation for future work, the practical use of the energy balance to enable blast designs which direct the available energy into the desired work and hence control the energy split between fracture energy, kinetic energy and radiated seismic energy, resulting in a more efficient use of the explosive energy. The present work assesses to some extent the feasibility of this energy approach, aiming at establishing, through new data and a thorough revision of the published work on the matter, the fraction of explosive energy transferred to the rock in its various components, with particular attention to their variability and the reasonable ranges that could be expected in quarry blasting.

The basic theory and experimental background for the determination of some of the energy components in rock blasting are described first. These are then applied to ten production blasts and one single, confined (without rock movement) blasthole. Eight of the production blasts and the confined shot were conducted in a limestone quarry (El Alto, Spain); two more production blasts were monitored in an amphibolite quarry (Eibenstein, Austria). Seismographs, high-speed video camera and fragmentation monitoring systems were used to measure the seismic field, the initial velocity of the blasted rock face and the fragment size distribution curve, respectively, from which the various energy terms are calculated. Vibrations were measured in the single confined hole.

2. The energy balance of blasting

The energy released by the explosive, borne in the detonation products upon completion of the chemical reaction, is converted into heat and work to the surroundings according to the first principle of thermodynamics. Some of these forms become apparent during the blast, namely: (a) the fracture work, that ultimately appears as new surface in the rock fragments; (b) the work transferred as shock wave into the rock, that propagates as plastic and ultimately elastic waves, appearing as seismic wave or ground vibration; and (c) the work to displace the rock and form the muckpile, that appears as kinetic energy imparted to the rock.

This energy partition is to some extent arbitrary and is based on the end effects of the blasting. For instance, part of the fracture work is in its first stage intimately connected to the shock wave flow in the vicinity of the hole and, in the later stages, also to the rock movement, which begins as the fractures burst open. Such a partition is, however, convenient inasmuch as the physical magnitudes related with each component can be measured. Other energy transfer takes place, in a less apparent way, as follows: (a) expansion work of the fractures, that is absorbed as elastic and plastic deformation of the rock in the surface of the fractures as they are penetrated by the gases; (b) heat transferred to the rock from the hot detonation products; and (c) heat and work conveyed as enthalpy of the gases venting to the atmosphere through open fractures and stemming.

The energy balance of the blast can thus be expressed by [2]:

$$E_E = E_F + E_S + E_K + E_{NM}, \tag{1}$$

where E_E is the explosive energy, E_F is the fragmentation energy, E_S is the seismic energy, E_K is the kinetic energy, and E_{NM} is the energy forms not measured. The terms fragmentation, seismic and kinetic efficiency are used hereafter for the ratios of the respective energies to the explosive energy.

2.1. Fragmentation energy

A specific amount of energy is required to create a new fracture surface [10]; let this energy, per unit surface, be G_F. The fragmentation energy can thus be calculated by

$$E_F = A_F G_F, \tag{2}$$

where A_F is the surface area of the fragments generated by the blast. The specific fracture energy G_F can be calculated from experimental fragmentation tests under a controlled energy input by means of mechanical comminution, leading to the Rittinger coefficient (a crushing efficiency, the surface area created per unit energy input), or derived from material properties of the rock—the fracture toughness and the elastic modulus. The first method involves millions of fractures in the rock, while the fracture toughness is obtained from tests in which only one fracture is formed. For the estimation of the fragmentation efficiency by blasting, where a great amount of fines is produced, the inverse of the Rittinger coefficient is used here as the specific fracture energy. The crushing efficiency concept and Eq. (2) assume that such efficiency is constant for all fragment sizes.

The surface area of the fragments may be estimated from the muckpile size distribution, assuming spherical or cubic particles of diameter or edge length x [3]:

$$A = 6V \int_0^\infty \frac{f(x)}{x}\,dx, \tag{3}$$

where V is the volume of the fragmented rock and $f(x)$ is the density function of the fragment size distribution in volume. An incremental version of Eq. (3) may be used when the size distribution curve is known in a discontinuous form (as this is usually the case) with the material grouped in classes of volume fractions p_k:

$$p_k = \int_{x_k^I}^{x_k^S} f(x)\,\mathrm{d}x = P(x_k^S) - P(x_k^I), \tag{4}$$

where $x_k{}^I$ and $x_k{}^S$ are the mesh size limits of class k ($x_k^S = x_{k+1}^I$) and $P(x)$ is the cumulative size distribution of the fragments. Eq. (3) can be written as a sum of the integrals for each class:

$$A = 6V \sum_{k=1}^{C} \int_{x_k^I}^{x_k^S} \frac{f(x)}{x}\,\mathrm{d}x, \tag{5}$$

where C is the number of classes. The function $f(x)$ is not known, but integrals for each class are, via Eq. (4). A mean value f_k for each class can be calculated from its integral value:

$$f_k = \frac{p_k}{(x_k^S - x_k^I)}. \tag{6}$$

The integrals in Eq. (5) can be approximated using the f_k values:

$$\begin{aligned} A &= 6V \sum_{k=1}^{C} \int_{x_k^I}^{x_k^S} \frac{f_k}{x}\,\mathrm{d}x = 6V \sum_{k=1}^{C} \frac{p_k}{(x_k^S - x_k^I)} \int_{x_k^I}^{x_k^S} \frac{\mathrm{d}x}{x} \\ &= 6V \sum_{k=1}^{C} \frac{p_k}{(x_k^S - x_k^I)} \ln \frac{x_k^S}{x_k^I}, \end{aligned} \tag{7}$$

or,

$$A = 6V \sum_{k=1}^{C} \frac{p_k}{x_k}, \tag{8}$$

where x_k is the logarithmic mean of the size limits of class k:

$$x_k = (x_k^S - x_k^I)/\ln(x_k^S/x_k^I). \tag{9}$$

The in situ area of the natural discontinuities of the rock mass, though small compared to the surface area created in the blast, is subtracted from the muckpile fragments area in order to obtain the newly formed surface area [3,11]. The area of fragments originated from the blast is

$$A_F = A - A_{IS}, \tag{10}$$

where A_{IS}, is the in situ specific area.

2.2. Seismic energy

The energy transferred to the rock in the form of seismic wave is calculated as the integral of the energy flow past a control surface at a given distance from the blast. The energy flux (the power or rate of work, per unit area) is the scalar product of the stress at the surface and the particle velocity [12]:

$$\Phi = \vec{t} \cdot \vec{v}, \tag{11}$$

where $\vec{t}$ and $\vec{v}$ are the stress and particle velocity vectors, respectively. The stresses are obtained from the stress tensor $\boldsymbol{\tau}$ by the Cauchy formula,

$$t_j = \tau_{ij} n_i, \tag{12}$$

where the summation convention is used. The energy flux is then:

$$\Phi = \tau_{ij} n_i v_j. \tag{13}$$

In order to relate the velocities, known from the seismographs readings, with the stresses, some assumptions must be made. If the seismic wave is considered as longitudinal spherical wave in an infinite homogeneous medium, the stress tensor in its principal components is, in spherical coordinates [13]:

$$\begin{aligned} \tau_{11} &= (\lambda + 2\mu)\frac{\partial u_1}{\partial r} + 2\lambda \frac{u_1}{r}, \\ \tau_{22} &= \tau_{33} = \lambda \frac{\partial u_1}{\partial r} + 2(\lambda + \mu)\frac{u_1}{r}, \quad \tau_{ij}(i \neq j) = 0, \end{aligned} \tag{14}$$

where u_1 is the radial component of the particle displacement and r is the distance from the source; λ and μ are the Lamé constants. For a spherical surface coincident with the wave front, its normal unit vector in the principal axes is (1,0,0). Substituting Eqs. (14) and (13) yields:

$$\Phi = \left[(\lambda + 2\mu)\frac{\partial u_1}{\partial r} + 2\lambda \frac{u_1}{r}\right] v_1, \tag{15}$$

where v_1 is the radial component of the particle velocity. The total power across the surface of radius r is, assuming a constant flux in it:

$$P = 4\pi r^2 \Phi. \tag{16}$$

Thus, the energy is

$$\begin{aligned} E_{S1} = \int_0^\infty 4\pi r^2 \Phi\,\mathrm{d}t &= 4\pi r^2 \\ &\times \int_0^\infty \left[(\lambda + 2\mu)\frac{\partial u_1}{\partial r} + 2\lambda \frac{u_1}{r}\right] v_1\,\mathrm{d}t. \end{aligned} \tag{17}$$

The velocity is measured by vibration monitoring conducted on the ground surface; the radial component may be assumed equal to the usually called longitudinal velocity in seismic measurements. The particle displacements can be calculated by the time integral of the velocity records:

$$u_1(t) = \int_0^t v_1(t)\,\mathrm{d}t. \tag{18}$$

The spatial derivative of the displacement can be approximated by the relation:

$$\frac{\partial u}{\partial r} = -\frac{v}{c}, \tag{19}$$

where c is the wave velocity. Eq. (19) applies when $v \ll c$, which is the case here. The equation for the calculation of

the seismic energy is, finally:

$$E_{S1} = 4\pi r^2 \int_0^\infty \left[-(\lambda + 2\mu)\frac{v_1^2}{c_L} + 2\lambda \frac{u_1 v_1}{r} \right] dt, \quad (20)$$

where the longitudinal wave velocity c_L is used. The time integral of the second summand of the integrand is nil for a harmonic wave; in our seismic records, it is usually less than 0.05% of the integral, so that it can be neglected without much error. Then:

$$E_{S1} = -4\pi r^2 \rho c_L \int_0^\infty v_1^2 \, dt, \quad (21)$$

where the relation $c_L^2 = (\lambda + 2\mu)/\rho$ has been used, ρ being the rock density. The negative sign in Eq. (21) indicates that the energy is leaving the control sphere (hence reducing the total energy in it). Eq. (21) is also obtained for a plane longitudinal wave, which can approximate a spherical wave at large radii.

The seismic energy, as calculated by Eqs. (20) or (21), is that of a spherical or plane P-wave in an elastic medium having as radial component v_1 of the particle velocity, the longitudinal component measured in the field. Assuming that the transverse and vertical components of the velocity (v_2 and v_3) belong to transverse waves, and using the plane wave approximation, the following expressions are readily obtained:

$$E_{S2} = -4\pi r^2 \rho c_T \int_0^\infty v_2^2 \, dt; \quad E_{S3} = -4\pi r^2 \rho c_T \int_0^\infty v_3^2 \, dt. \quad (22)$$

Adding Eq. (22) to the P-wave energy (Eq. (21)) and using the absolute value gives

$$E_S = 4\pi r^2 \rho \left[c_L \int_0^\infty v_1^2 \, dt + c_T \int_0^\infty (v_2^2 + v_3^2) \, dt \right]. \quad (23)$$

Eq. (23) is usually further simplified [2,3,9], using a unique wave velocity, to

$$E_S = 4\pi r^2 \rho c_L \int_0^\infty v^2 \, dt, \quad (24)$$

where v is the magnitude of the vector sum of velocities, $v^2 = v_1^2 + v_2^2 + v_3^2$. If there is a sufficient characterization of the material so that the longitudinal and transverse velocities are known, and three-components records are available, Eq. (23) should be preferred. This is used in the present work.

The measured velocity functions do not belong to spherical waves from a point source, but from a number of line (or cylindrical) sources at varying distances from the measuring point. They are a composition of longitudinal, transverse and surface waves resulting from reflections and refractions at the stratification, joints and the free surfaces—the bench face and the ground surface. As the composed wave comes from different sources, the assumption that each of the three components belongs to separate longitudinal or transversal waves is obviously unrealistic. Even for the direct waves, the radial component of the velocity measured (pointing towards the center of the blast) is not collinear with the directions to the different blastholes. Finally, the domain boundary is a hemisphere closed by a circle; the use of a sphere surface area in Eq. (16) and subsequent rests on the assumption that what was found at the position of the measurements represents the seismic field in a complete sphere. As the velocity was measured on the surface, not a good sample of velocity in an infinite medium, some of the energy is reflected downwards, resulting in an outgoing flow smaller than what would be encountered with the gauge embedded in the medium at depth. Thus, Eq. (23) is only a rough approximation to the seismic energy from a blast. It is a simple solution encompassing many simplifying assumptions for a very intricate problem.

2.3. Kinetic energy

The kinetic energy is calculated from measurements of initial velocity of the rock face at different heights along the highwall, $V_0(y)$. High-speed film and radar measurements [2] showed that the face velocity distributions for many blasts were relatively narrow, and the rocks behind the face generally move in unison with the face (this behavior is typical of competent brittle rocks [14]). Assuming that lateral variations of velocity are of second order to the vertical variations, i.e., that the velocity of the entire rock mass is constant in a horizontal section of the burden, the kinetic energy E_K of the rock displaced by a blasthole is

$$E_K = \frac{1}{2} S B_h \int_0^H \rho(y) V_0^2(y) \, dy, \quad (25)$$

where a variable rock density has been considered, $\rho(y)$, to account for lithology variations along the height, assuming a horizontally layered rock (this is used for El Alto, where overburden and rock are differentiated). H is the bench height, S is the spacing between holes and B_h is the mean horizontal burden, obtained from the face profile.

3. Measurements and calculation of the energy components

3.1. Description of the blasts

El Alto quarry belongs to Cementos Portland Valderrivas, a cement and aggregate producer located in the province of Madrid, Spain. The quarry produces 2.25 Mt/yr of limestone and marl. The deposit is of Miocene age and lacustrine origin. The geology is simple and essentially uniform. In the upper 2–6 m, there is an overburden of weathered clayey marl of sandy nature (with a maximum particle size of 14 mm) and low cohesion, underlying a clayey soil of some tens of centimeters. The limestone formation below this has a thickness of 12–19 m; the bedding planes are horizontal or subhorizontal and crossed by some nearly vertical faults. The floor of the limestone is clay (*greda*) that is usually not mined. The quarry is mined in one bench.

Table 1
Rock properties

	Limestone, El Alto	Amphibolite, Eibenstein	References
Density, kg/m^3	2560	2950	[16]
Tensile strength, MPa	7.6	7.5	[16]
Elastic modulus, GPa	64	83	[16]
Poisson's ratio	0.26	0.22	[16]
Rittinger coefficient, cm^2/J	58	34	[17]
In-situ block size, 63% pass, m	3.01	2.63	[15]
In-situ block size, uniformity index	2.86	2.13	[15]
p-wave velocity, in situ rock mass, m/s	2994	2450	[18,19]
p-wave velocity, laboratory specimen, m/s	4314	5726	[15]

Eibenstein quarry is owned by Hengl Bitustein, an aggregate producer in Austria. The quarry produces 250 kt/yr of marble and amphibolite. The formation is a metamorphic body including amphibolite, schist, micaschist and marbles. All the deposit is heavily folded and faulted with a complex structure; schistosity and foliation are present in all rock types. The quarry is mined in several benches.

A comprehensive rock mass description of both quarries has been reported by Hamdi and du Mouza [15]. The main properties of the rocks are given in Table 1.

The main characteristics of the blasts are shown in Tables 2 and 3. The numbering of the blasts used by the quarries has been retained (a correlative number and year in El Alto; bench level and correlative number in Eibenstein; CB2 is the confined shot, fired in El Alto). The mean and standard deviation (following the ± sign) of the values measured hole per hole are given for some of the

Table 2
Characteristics of the blasts, geometrical

Blast no.	Site	N	i (deg.)	H (m)	h_{ob} (m)	J (m)	B (m)	B_h (m)	S (m)	S/B	Vol-t (m^3)	Vol-r (m^3)
CB2	El Alto	1	0	16.5								
15/02	El Alto	22	6	19.6±1.1	3.0	2.7	5.5±0.3	5.5	5.9	1.07	640	542
29/02	El Alto	21	6	19.9±2.6	3.4	1.1	4.9±0.4	4.9	6.0	1.22	588	488
37/02	El Alto	26	6	19.5±2.5	2.4	2.2	5.0±0.5	5.0	5.8	1.16	569	499
43/03	El Alto	10	6	18.0±1.0	1.9±0.5	1.5	4.5±0.3	4.5	6.5±0.1	1.44	529	474
45/03	El Alto	10	6	16.3±0.4	3.9±0.5	1.6	4.6±0.4	4.6	6.5±0.1	1.41	490	373
50/03	El Alto	10	6	18.2±1.0	2.2±0.5	1.7	4.6±0.1	4.6	6.6±0.2	1.43	556	488
54/03	El Alto	11	6	18.5±0.3	2.3±0.5	2.7	5.0±0.4	5.0	6.4±0.1	1.28	595	521
58/03	El Alto	10	6	17.1±0.6	3.4±0.7	1.5	4.4±0.1	4.4	6.4±0.4	1.45	484	388
420-11	Eibenstein	7	21	10.1±0.4	0	1.5	3.6±0.7	3.9	3.3±0.1	0.92	129	129
440-04	Eibenstein	9	19	12.9±0.6	0	0.1	4.1±0.4	4.3	3.3	0.80	185	185

N: number of holes; i: hole inclination (nominal in El Alto, measured in Eibenstein); H: bench height (hole length for the confined shot); h_{ob}: overburden thickness; J: subdrill; B: burden; B_h: horizontal burden; S: spacing; S/B: spacing-to-burden ratio; Vol-t: Total volume blasted per hole; Vol-r: Volume of rock (excluding overburden) blasted per hole.

Table 3
Characteristics of the blasts, explosives

Blast no.	Expl.	M_{ET}, kg		E_{ET}, W_u (MJ)	E_{ET}, Q (MJ)	M_{EH}, kg		q (kg/m^3)	E_{EH}, W_u (MJ)	E_{EH}, Q (MJ)	t (ms)
		Cartr.	Bulk			Cartr.	Bulk				
CB2	G2/AN	2.5	75	203	302	2.5	75		203	302	—
15/02	G2/AL	550	4664	15524	25243	25	212±35	0.37	706	1147	84-N
29/02	G2/AL	546	4326	14523	23560	26±1	206±48	0.39	692	1122	67-N
37/02	G2/AL	650	5798	19181	31243	25	223±26	0.44	738	1202	67-N
43/03	G2/AL	250	2000	6706	10883	25	200±13	0.43	671	1088	67-E
45/03	G2/AL	250	1830	6210	10044	25	183±25	0.42	621	1004	17-E
50/03	G2/AL	250	2130	7085	11523	25	213± ±13	0.43	709	1152	30-E
54/03	G2/HA	275	2849	10421	15299	25	259±17	0.48	947	1391	67-E
58/03	G2/HA	250	2100	7846	11470	25	210±10	0.49	785	1147	67-E
420-11	GD/AD	255	125	1302	1633	36.4±3.1	17.8±6.4	0.42	186	233	20-e
440-04	GD/AD	267	275	1731	2263	29.7±9.7	30.6±10	0.33	192	251	20-e

M_{ET}: total mass of explosives; E_{ET}: total explosive energy, useful work (W_u) or heat of explosion (Q); M_{EH}: mass of explosives per hole; q: powder factor; E_{EH}: explosive energy per hole; t: in-row delay and type of initiation; N: non-electric, E: electronic, e: electric.

parameters. Burden B for each hole was obtained from laser profiles of the bench face. Bench height was also obtained from these profiles.

Blasts in El Alto were carried out in La Concha, one of the two pits of the quarry; blasts numbers 29/02, 37/02, 45/03, 54/03 and 58/03 belonged to the same area while blasts 15/02, 43/03 and 50/03 were in different areas of the pit. In Eibenstein, blasts 420-11 and 440-04 were located in the levels 420 and 440 of the quarry respectively.

The blasthole diameter was 142 mm in El Alto and 92 mm in Eibenstein. All production blasts consisted of a single row of blastholes. One charge per hole was blasted in all rounds, except in blast 15/02, where two decks were fired separated by 1 m of stemming with 50 ms top-bottom delay. The delay and the detonator type used in each blast are given in Table 3. The delay in blast 37/02 was basically 67 ms, although it was variable along the blast since some of the holes were decked; the holes with intermediate stemming are not included for the statistics given in Table 3.

Gelatine cartridges were used as bottom charge (Goma 2 ECO, abbreviated G2 in Table 3, and Danubit 4, abbreviated GD); aluminized ANFO (Alnafo, abbreviated AL), a high-density aluminized ANFO (abbreviated HA) and standard ANFO (Nagolita, abbreviated AN, and Dap 2, abbreviated AD) were used as column charges. Down-hole initiation was used in El Alto. Detonating cord side initiation was used at Eibenstein. Table 4 shows the properties of these explosives. Detonation velocities were measured in all blasts in one or two holes.

The explosive energy can be rated in different ways, either from thermodynamic codes or from experimental measurements such as the underwater test [20,21] and the cylinder test [22]. Lacking of a universal test for the determination of the explosive energy, which largely depends on the principle of the test itself, thermodynamic calculations are generally accepted means of assessing the energy of explosives. The energy of the explosives used in El Alto has been calculated using the W-Detcom code [23,24]; the heat of explosion at constant volume, E_Q, and the useful work to an expansion cut-off pressure of 100 MPa, E_{Wu}, have been used as energy values. The BKW-S equation of state [25,26] has been used for the calculations. For the explosives used in Eibenstein, the heat of explosion given by the manufacturer [27] is the only available figure of explosive energy since their exact compositions are unknown. The useful work has been estimated for the gelatine and the ANFO used in Eibenstein assuming the same fractions of energy lost below 100 MPa as for the El Alto's gelatine and ANFO, respectively.

3.2. Fragmentation energy

The fragment size distribution was measured in both quarries using digital image analysis software applied to the images recorded by a camera installed at the hopper of the primary crusher.

The procedure used to obtain the fragmentation in El Alto is described in [28]. Basically, 20 good-quality photographs (good lighting and full bin) were randomly sampled from all the photographs from a blast. The photos were analyzed with the *Split® Desktop* code [29,30] with a fines correction factor calibrated from large-scale muckpile sieving data. The main errors committed in the automatic delineation, i.e., over-divided large rocks and fines areas, were corrected manually as required; a robust detection of outlier photographs was performed using the median deviation about the median. The overburden in El Alto complicates the assessment of the fragmentation, as it contributes to the fines present in the muckpiles; an adjusted fines correction factor was used, variable with the amount of fines originating from the loose overburden (natural fines). The fragment size distributions of the limestone from blasting were obtained by subtracting the fraction of natural fines (estimated as the ratio of the overburden thickness to the bench height) from the raw muckpile fragmentation curves. This was done using laboratory screening data of the overburden material and of the muckpile fine fraction. It was assumed that the fines tail of the limestone has the same distribution in all the blasts for sizes below 14 mm (maximum size of the overburden), following the natural breakage characteristic principle [31,32].

In Eibenstein, all photos available per blast were analyzed in an automatic mode and no manual correction was done. Fragmentation was measured with the image analysis code *Fragscan* [33], calibrated from a muckpile

Table 4
Properties of the explosives

Name	Type	Manufacturer	Density (kg/m^3)	VOD (m/s)	E_{Wu} (kJ/kg)	E_Q (kJ/kg)
Nagolita	ANFO	UEE	800	3941[a]	2591	3893
Dap 2	ANFO	Istrochem	800	3867 ± 85	2529	3800
Alnafo	ANFO + Al	UEE	800	4029 ± 93	2918	4930
High density Alnafo	ANFO + Al	UEE	950	3424 ± 98	3322	4975
Goma 2 ECO	Gelatin	UEE	1450	6321 ± 118[b]	3480	4090
Danubit 4	Gelatin	Istrochem	1450	5933 ± 197	3871	4550

[a]One-shot value.
[b]Values include data for 65 and 85 mm diameter cartridges.

sieving in order to overcome the problem of fines detection [34,35]. The Swebrec function [36] was used for extrapolating the measurements outside the range of resolution of the image analysis, 63 mm, down to 10 mm. Further extrapolation would be risky, as a second function (i.e., a bimodal distribution) would probably be required.

The size distribution curves are plotted in Fig. 1. The smallest sizes of the curves are 0.25 mm for El Alto and 10 mm for Eibenstein (downwards extrapolations are shown in Fig. 1 as dashed lines). El Alto's data corresponds to broken limestone (natural fines discounted). The kink at 14 mm is the junction of the fines tail and the fragmentation measured with *Split*.

Eq. (8) is used for the calculation of the surface area of the fragments, except for the finer class, $[0, x_{\min}]$; $x_{\min}$ is 0.25 mm in El Alto and 10 mm in Eibenstein. For that class, a Rosin–Rammler (or Weibull) cumulative distribution is assumed:

$$P(x) = 1 - e^{-(x/x_c)^n}; \quad 0 \leqslant x \leqslant x_{\min}, \tag{26}$$

where x_c and n are the parameters of the Rosin–Rammler–Weibull distribution (characteristic size and uniformity index, respectively). Following the technique of [29], the two parameters are determined from the last two known data points. The probability density function is

$$f(x) = \frac{n}{x_c^n} x^{n-1} e^{-(x/x_c)^n}; \quad 0 \leqslant x \leqslant x_{\min}. \tag{27}$$

The contribution to the specific surface area of the undefined fines tail is, using Eq. (27) in Eq. (3) and integrating between 0 and $x_{\min}$:

$$\frac{A_{\text{tail}}}{V} = 6\int_0^{x_{\min}} \frac{f(x)\,dx}{x} = 6\int_0^{x_{\min}} \frac{n}{x_c^n} x^{n-2} e^{-(x/x_c)^n}\,dx = \frac{6}{x_c}\gamma\left[1 - \frac{1}{n}, \left(\frac{x_{\min}}{x_c}\right)^n\right], \tag{28}$$

with γ being the lower incomplete Gamma function. This approach was followed successfully for El Alto data, as the lower part of the size distribution is reasonably of Rosin–Rammler–Weibull type, but proved unfeasible for the Eibenstein distributions. This is due to the use of the Swebrec function in Eibenstein, so that the Rosin–Rammler–Weibull functions obtained for the lower part of the distribution have a very low uniformity parameter n (less than 1), which makes the integral in Eq. (28) divergent. Hence, the Swebrec functions were extended down to 0.25 mm (the dashed portion of the curves in Fig. 1) in order to make the calculations comparable with El Alto, although such size range is probably beyond the validity of the Swebrec function. The surface area of the lower class [0, 0.25 mm] was in this case calculated as one more summation term of Eq. (8), with a mean size $x_k = 0.125$ mm. Comparing the two methods of calculation for El Alto curves, the latter results in an underestimation of the total fragmentation energy of about 3–7% with respect to the integral formulation.

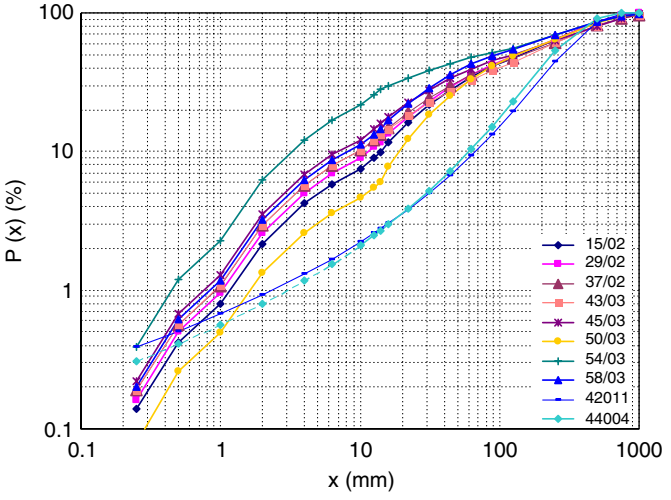

Fig. 1. Size distribution curves.

Table 5 shows, for each blast, the specific surface area of the fragments, A/V, and the new specific area, A_F/V (by subtraction of the in-situ block size area, calculated from the Rosin-Rammler—Weibull parameters in Table 1: 2.8 and 3.8 m^2/m^3 for El Alto and Eibenstein respectively). The fragmentation energies per hole, E_F, are obtained from the new area, the volume of rock blasted per hole in Table 2 (column Vol-r) and the specific fracture energy (inverse of the Rittinger coefficient in Table 1). The energies and the fragmentation efficiencies, η_F, with respect to both ratings of explosive energy, useful work and heat of explosion, are

Table 5
Fragmentation energy and efficiency

Blast no.	A/V (m^2/m^3)	A_F/V (m^2/m^3)	E_F, per hole (MJ)	η_F, W_u (%)	η_F, Q (%)
15/02	382.2	379.4	35.4	5.0	3.1
29/02	432.1	429.4	36.1	5.2	3.2
37/02	488.7	486.0	41.8	5.7	3.5
43/03	483.6	480.9	39.3	5.9	3.6
45/03	561.9	559.2	35.9	5.8	3.6
50/03	259.8	257.1	21.6	3.1	1.9
54/03	934.8	932.0	83.8	8.8	6.0
58/03	529.0	526.3	35.2	4.5	3.1
420-11	285.7	281.9	10.7	5.7	4.6
440-04	246.5	242.7	13.2	6.9	5.3

also listed in Table 5. The efficiencies in Eibenstein are not outliers to the distribution of efficiencies in El Alto. The range of efficiencies is 1.9–6.0% of the heat of explosion and 3.1–8.8% of the useful work.

The mean fragmentation efficiency in El Alto is 5.5% and 3.5% with respect to useful work and heat of explosion, respectively. In Eibenstein, it is 6.3% and 4.9%.

3.3. Seismic energy

The seismic field was measured with Multiseis Plus seismographs of Vibra-tech. The ranges of velocity and frequency are 254 mm/s and 2–300 Hz respectively with an accuracy of 3% at 15 Hz. The seismographs were coupled to the ground surface in El Alto by excavating a shallow hole to remove some tens of centimetres of the upper layer of soil and the devices were spiked in the bottom. Sandbags (ANFO bags filled with sand) were fitted in the hole so that they were sort of fixing the mount not only in the vertical movement but also horizontally. In Eibenstein, the seismographs could not be spiked to the ground and they were placed in a shallow hole, of depth slightly larger than the seismograph height, covered with gravel and the surrounding earth compacted. Given that this mounting could not be optimal [37,38], care was exercised to evaluate the recorded signals by inspection of the time records and the frequency analysis. Where most of the energy was packed at very low frequencies in one or more components of the velocity, the measurement was rejected [39]. This happened in two measurements. Fig. 2 shows two examples of acceptable records and the two records rejected.

The distances of the seismographs to the blast (average of distances to each of the holes) were kept, as much as possible, similar from blast to blast. The distances were 51.8 m for the confined shot and a mean and standard deviation of 65.5 and 4.4 m, respectively for the production blasts in El Alto; in Eibenstein the mean and standard deviation were 36.9 and 1.3 m, respectively. The seismographs were placed around the block to be blasted in both top and floor levels as close as possible to the blast, but to a distance large enough so as not to be too close to any of the holes. The sensors in the bottom level were placed slightly farther in order to allow room for the muckpile. The sensors in El Alto were located around the blast at approximately even angles. The confined blasthole, CB2, was drilled in the upper level of the quarry, far from the bench; all measurements were made in that level. The berms at Eibenstein were narrow, which restricted the position of the seismographs to directions close to the blastholes line. Fig. 3 shows two examples.

Table 6 shows the mean of the distances to the blastholes for each sensor unit, r and the peak vector sum particle velocity, PPVs. Data measured on the top and floor of the bench are shown separately.

Eq. (23) is calculated numerically from the seismic records' particle velocity data v_1 (longitudinal), v_2 (transverse) and v_3 (vertical); the integration step is the sampling interval, 1/1024 s, in all the records. The rock mass longitudinal wave velocities measured on-site (Table 1) are used. The transverse wave velocity used is obtained from the relation:

$$c_T = (\mu/\rho)^{1/2}, \tag{29}$$

where μ is determined from the in situ P-wave velocity used, the density and the Poisson's ratio in Table 1; El Alto limestone: $\mu = 7.44$ GPa; $c_T = 1705$ m/s; Eibenstein amphibolite: $\mu = 6.36$ GPa; $c_T = 1468$ m/s.

Seismic energy obtained at each seismograph's location is given in Table 6. Seismic efficiencies are obtained from the seismic energies and the total explosive energies given in Table 3.

The scatter of energies and efficiencies is in some cases large among sensors in the same blast; such dispersion is not unusual in seismic measurements. Given that the range of distances in each site was very narrow, no significant functional relationship of the seismic energy efficiency and the distance can be drawn (see Fig. 4), thus all energies in each site can be treated together without an attenuation correction for distance. Using lognormal distributions for the seismic efficiencies (the hypothesis of lognormality cannot be rejected at a 95% confidence level), their means in El Alto are different in the top and floor levels at a 95% confidence level. They are 2.5% in the top and 1.2% in the floor with respect to the heat of explosion. The mean seismic efficiency of the confined shot is 8.6% with respect to the heat of explosion, more than three times the mean value of production blasts in the top level. Though the distance of measurement in the confined shot was about 20% shorter than in the production blasts, such a high energy value must be explained by the absence of interference between waves from different holes, the confinement of the charge and especially, according to Blair and Armstrong [40], the undamaged nature of the rock mass around the hole.

The efficiencies in the top and floor levels in Eibenstein (mean values of the lognormal distributions 1.1% and 0.7%, respectively) are not different at a 95% confidence level. Taking all values as one distribution, the mean efficiency in Eibenstein is 0.9% with respect to the heat of explosion. Table 7 gives a summary of the results.

3.4. Kinetic energy

A Motion Meter 1000 high-speed digital camera, of Redlake Imaging, was used, with a recording velocity of 250 frames per second. Wooden targets hanging on the bench face were used to determine the rock displacement and four fixed points with known coordinates were used as reference system. Fig. 5 shows a sketch of the set-up; details of the system used in each quarry are given in [41].

The targets were placed approximately in front of the explosive column. In blast 15/02 with two decks, the targets were located in front of the upper deck area. Two targets were used in Eibenstein and in blasts 15/02, 29/02 and

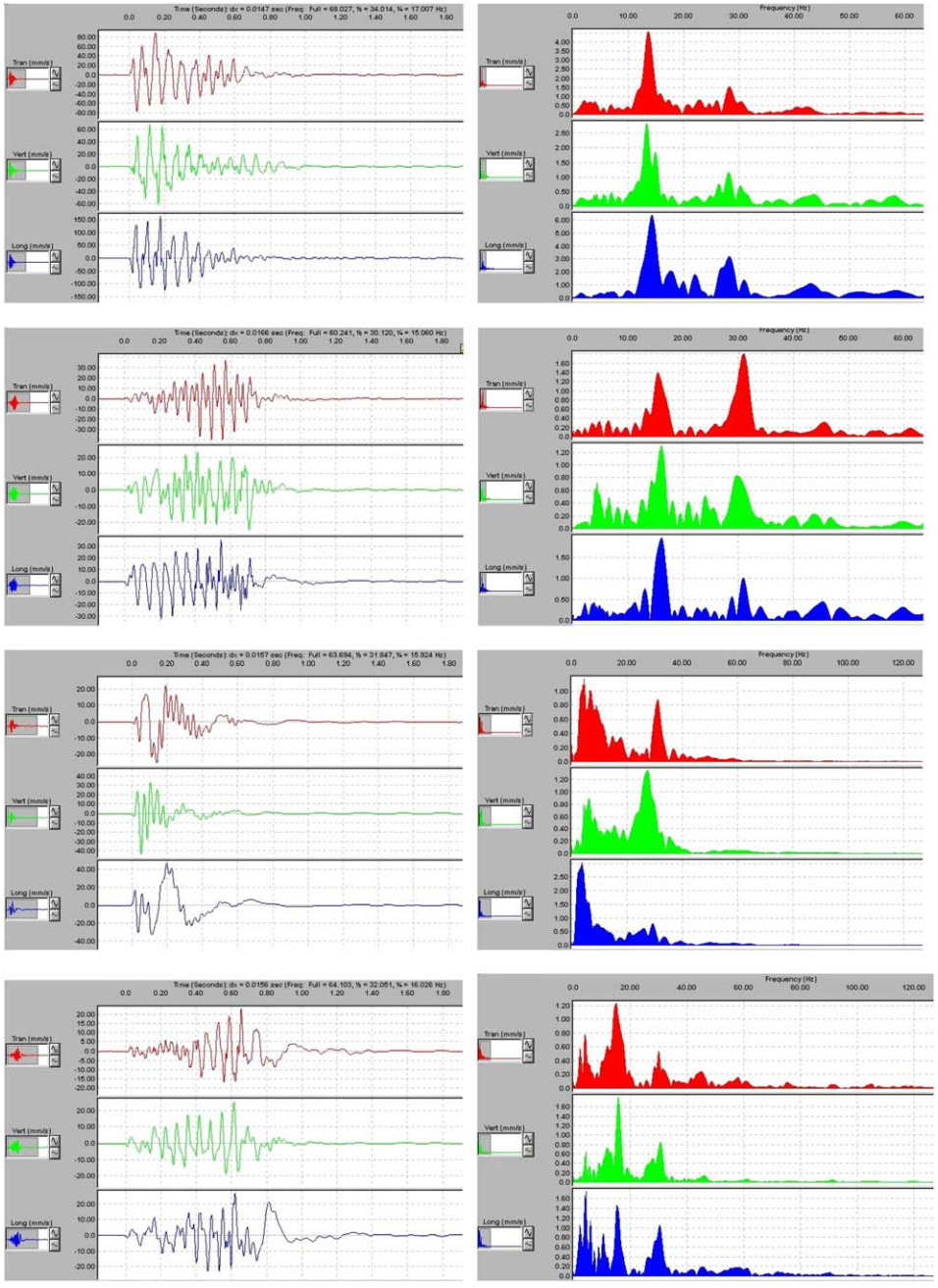

Fig. 2. Sample seismograms and frequency spectra. From top to bottom: blast 54/03, units 7640 and 6783 (acceptable records); blast 50/03, unit 7837 and blast 58/03, unit 7101 (rejected records).

37/02 of El Alto. In the other five blasts monitored in El Alto, the number of targets were increased to four (though not all of them could be tracked in every blast). The positions of the targets (hole in front of which they were located and height from grade) are given in Table 8. The targets are numbered from the floor to the top of the bench face. As the features of the rock movement in a vertical section depend basically on the local geometrical and charging values, more than on the average values of the whole blast, the precise drilling and charging data of the blasthole behind the targets are used for the calculation of the kinetic energy term. These are given in Table 8.

Motion Tracker™ 2D software [42] was used to obtain the raw path of the targets. The initial velocity of the targets, listed in Table 8, is obtained from a trajectory model in which the two components of the initial velocity are modified until the calculated trajectory best-fits the measured flight points [41].

In our measurements, the velocity as a function of the height is known for a maximum of four values and in many cases for only two. A sound, statistically significant, fitting of a function $V_0(y)$ to be used in Eq. (25) is not possible for most of the blasts; an average velocity of the values measured for each blast has thus been used. Eq. (15)

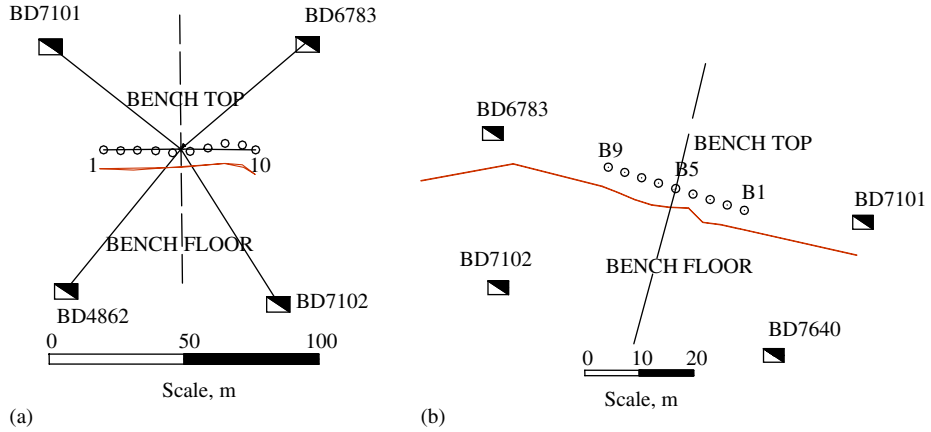

Fig. 3. Sample seismograph location. (a) Blast 58/03 (El Alto). (b) Blast 440-04 (Eibenstein).

Table 6
Basic vibration data and seismic energy

Blast no.	Bench top						Bench floor					
	Unit #	r (m)	PPVs (mm/s)	E_S (MJ)	η_S, W_u (%)	η_S, Q (%)	Unit #	r (m)	PPVs (mm/s)	E_S (MJ)	η_S, W_u (%)	η_S, Q (%)
CB2	7640	51.8	56.3	30	14.6	9.8						
	7102	51.8	53.8	20	10.0	6.7						
	7101	51.8	42.9	28	14.0	9.4						
15/02	7102	65.6	51.5	416	2.7	1.6	7101	77.9	26.7	92	0.6	0.4
29/02	7101	60.4	94.6	507	3.5	2.2	7102	66.1	89.2	338	2.3	1.4
	6783	61.3	93.4	358	2.5	1.5	7640	66.3	46.4	225	1.6	1.0
37/02	7101	61.5	102	479	2.5	1.5	6783	69.8	43.8	226	1.2	0.7
	7640	63.6	138	450	2.3	1.4	7102	62.5	36.7	108	0.6	0.3
43/03	7101	69.1	36.0	60	0.9	0.6	4862	68.5	53.7	327	4.9	3.0
	7640	60.6	95.9	383	5.7	3.5	6783	68.5	90.1	390	5.8	3.6
45/03	7101	61.0	146	203	3.3	2.0	6783	67.3	62.2	143	2.3	1.4
	4862	59.3	158	314	5.1	3.1	7640	66.1	47.1	98	1.6	1.0
50/03	7640	60.8	150	467	6.6	4.1	7102	68.1	31.1	31	0.4	0.3
	7837	Rejected					7101	69.4	62.1	59	0.8	0.5
54/03	7640	62.6	169	937	9.0	6.1	7102	67.5	29.6	61	0.6	0.4
	6783	58.5	41.1	78	0.8	0.5	7101	69.8	36.8	105	1.0	0.7
58/03	6783	63.3	100	310	4.0	2.7	7102	69.7	42.5	133	1.7	1.2
	7101	Rejected					4862	68.6	54.7	234	3.0	2.0
420-11	7101	34.9	74.9	20	1.5	1.2	7102	38.5	41.0	9	0.7	0.5
	6783	36.7	31.9	6	0.4	0.3	7640	37.4	43.4	5	0.4	0.3
440-04	6783	36.2	63.9	13	0.7	0.6	7640	37.3	66.8	31	1.8	1.4
	7101	35.7	111	42	2.4	1.9	7102	38.8	54.7	14	0.8	0.6

becomes simply, for two layers of thickness h_1, h_2 and densities ρ_1, ρ_2:

$$E_K = \frac{1}{2}\bar{V}_0^2 SB_h(\rho_1 h_1 + \rho_2 h_2) = \frac{1}{2}\bar{V}_0^2 SB_h \times H\left[\rho_1 \frac{h_1}{H} + \rho_2\left(1 - \frac{h_1}{H}\right)\right]. \quad (30)$$

Burdens, spacings and bench heights in Table 8 are used. The overburden thicknesses, h_1, are given in Table 2. Two densities are considered in El Alto quarry, 1600 and 2560 kg/m^3, for overburden and limestone, respectively.

Table 9 shows the kinetic energies and efficiencies. Kinetic energy depends on the velocity squared so that moderate variations in velocity lead to important variations in the energy calculated thereof. The efficiencies in El Alto range from 3.3% to 10.3% with respect to heat of explosion and 5.3–16.5% with respect to the useful work. In Eibenstein, the results from the two blasts are quite different; the velocities measured in blast 420-11 are the highest ones in all blasts, due to the small local burden in the rock that was tracked (2.5 m horizontal burden; the average in that blast was 3.3 m), which resulted in an overcharged hole.

3.5. Uncertainty analysis

The uncertainties in the data measured have been estimated and from these, the uncertainties of the

calculated energies have been determined by error propagation through the formulae used in the calculations. The uncertainties of the measured variables are described, except where otherwise stated, by the relative standard error (standard deviation of the mean, expressed as a fraction of it). These have been calculated for each blast and the average values in all blasts used as the estimation of the uncertainty. The relative standard error of a variable x is denoted $\delta x/x$.

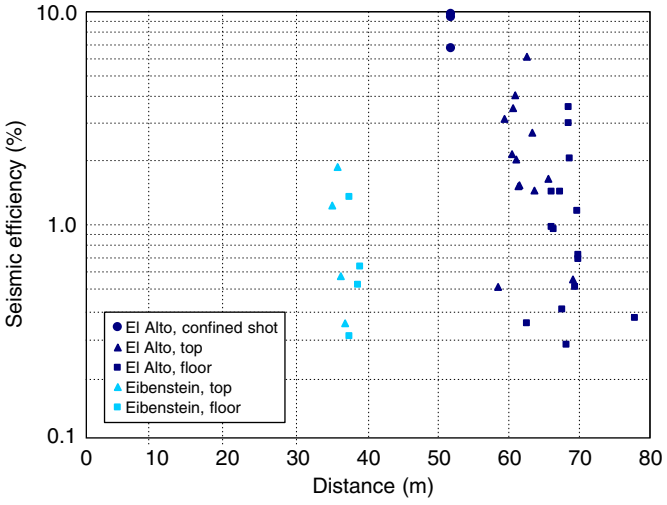

Fig. 4. Seismic efficiency with respect to distance.

Table 7
Summary of seismic efficiencies

	Useful work		Heat of explosion	
	Range	Mean	Range	Mean
El Alto, confined hole	10.0–14.6	12.9	6.7–9.8	8.6
El Alto, production blasts, top level	0.8–9.0	3.9	0.5–6.1	2.5
El Alto, production blasts, floor level	0.4–5.8	1.9	0.3–3.6	1.2
Eibenstein, both levels	0.4–2.4	1.1	0.3–1.9	0.9
All production blasts	0.4–9.0	2.5	0.3–6.1	1.6

1. Fragmentation energy. The basic equations are (2) and (8), where the volume of the rock is calculated from the burden, blasthole spacing and bench height. The fracture specific energy, G_F, is the slope of a linear fitting of energy vs. surface. The relative standard error, $\delta G_F/G_F$, is, from the data in [17], 0.044 for El Alto's limestone and 0.052 for Eibenstein's amphibolite. The higher value is used. For the burden, B, spacing, S and bench height, H, from Table 2: $\delta B/B = 0.024$, $\delta S/S = 0.018$, $\delta H/H = 0.006$. For the specific area of fragments, the error in the determination of percentages passing, p_k is estimated as the standard error of the percentages passing in the various photographs from a blast, averaged for all sizes and all blasts; $\delta p_k/p_k = 0.067$. It is assumed that this relative error also holds for the sum of p_k/x_k though the actual error of the sum is smaller by a factor of $C^{1/2}$, C being the number of the fragment classes; x_k are constant numbers. No consideration has been given to the uncertainty in the specific area of fragments when the fines tail is not conveniently resolved, as all calculations here have been done on the same basis. This should be deemed an important influential factor when analyzing data from various sources. The resulting relative standard error of the fragmentation energy is 0.09.
2. Seismic energy. The basic equation is (23). The error components are, for the distance, r, $\delta r/r = 0.019$, from the distances in Table 6. For the rock density, ρ, the higher value of the relative standard errors of Eibenstein and El Alto is $\delta\rho/\rho = 0.003$, from the laboratory data [16]. For the wave velocity, c, this was obtained by

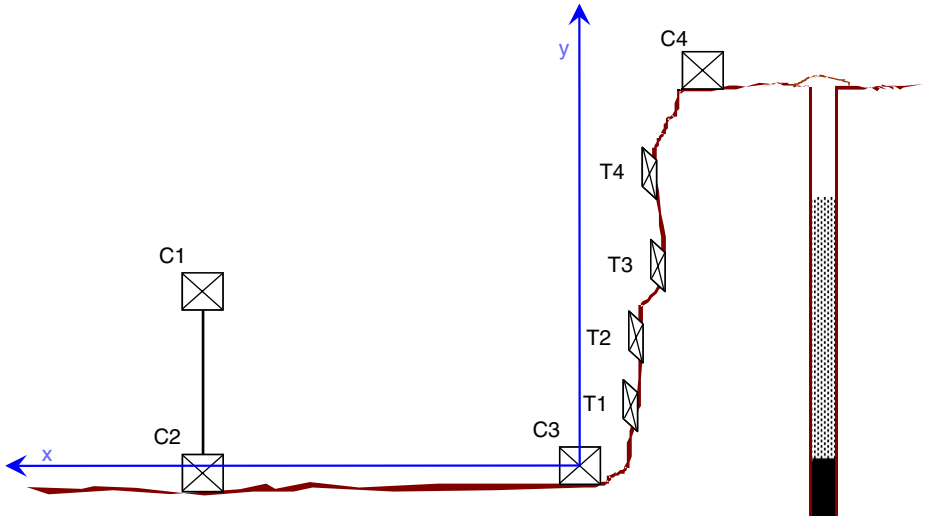

Fig. 5. Experimental set-up for measuring the face movement. C: control points; T: targets.

Table 8
Characteristics of the blastholes behind the targets and high-speed camera monitoring results

Blast no.	15/02	29/02	37/02	43/03	45/03	50/03	54/03	58/03	420–11	440–04
Hole no.	9	11	15	2	8	6	5	2	3	6
Bench height, m	20	17.2	17.2	16.7	15.7	17.9	18.5	16.5	10.4	12.8
Subdrill, m	4.8	−2.2	7.2	1.3	2.2	1.4	3.3	2.5	1.1	0.6
Mean (horizontal) burden, m	5.7	4.4	4.9	4.5	4.0	4.6	5.4	4.4	2.5	4.5
Spacing, m	5.9	6	5.8	6.4	6.4	6.7	6.4	6.4	3.3	3.3
Target height, m										
T4				11.1			12.8			
T3				8.9	9.1	11	11.3	8		
T2	16.1	10.3	11.6	6.4	5.5	6.3	9.6	5.5	5.9	9.4
T1	11.1	5.5	5.9	4.7		1.9	5.1	1.3	2.7	4.8
Initial velocity, m/s										
T4				10.4			6.4			
T3				12.8	7.3		9.2	14.8		
T2	9.8	10.3	6.5	9.6	9.2	9.8	8.7	16.1	18.9	9.3
T1	8.3	15.9	12.4	5.2		10	8.8	13	23.8	2.8
Explosives, kg										
Cartridged	25	25	25	25	25	25	25	25	35	35
Bulk	258	138	250	181	178	200	275	213	21	20
Energy, W_u, MJ/hole	840	490	817	615	606	671	1001	795	189	186
Energy, Q, MJ/hole	1374	783	1335	995	980	1088	1470	1162	239	235

Table 9
Average velocities, kinetic energies and efficiencies

Blast no.	Av. veloc. (m/s)	E_K, per hole (MJ)	η_K, W_u (%)	η_K, Q (%)
15/02	9.1	66.9	8.0	4.9
29/02	13.1	92.9	16.5	10.3
37/02	9.5	53.2	6.5	4.0
43/03	9.5	53.5	8.7	5.4
45/03	8.3	31.9	5.3	3.3
50/03	9.9	66.4	9.9	6.1
54/03	8.3	53.7	5.4	3.7
58/03	14.6	118.2	14.9	10.2
420-11	21.4	49.5	26.2	20.7
440-04	6.1	8.8	4.7	3.7

uphole surveys in both quarries and is the outcome of a division of distance by difference in time of arrival; using as distance standard error the same value as for r and 1 ms (a sampling frequency of 1024 samples per second was used) as absolute error for the time of arrival (i.e., $\sqrt{2}$ ms for the time difference), the relative standard error for the seismic velocity is 0.087 in El Alto and 0.24 in Eibenstein. The latter figure has been used as $\delta c/c$. One factor of uncertainty of major importance in the calculation of seismic energy is the use of P- or S-wave velocities, and whether these are taken from laboratory measurements or measured in situ, as both values can differ significantly. As with the area of fragments, we have not included this in the estimation of the uncertainty, though it should be considered when comparing energy values from different sources. For the time integrals of the particle velocity squared, the relative standard error of the particle velocity, calculated as the average of errors of the PPVs in each blast, is $\delta v/v = 0.21$. The integrals are calculated numerically as a sum of terms $v^2\delta t$, δt being the integration step. The relative standard error in the integral has been considered equal to that of v^2, $\delta v^2/v^2 = 0.42$. The resulting relative error for the seismic energy is 0.48.

3. Kinetic energy. The basic equation is (30). The error components for burden, spacing, rock density and bench height have been given above. The error in the rock ejection velocity is, from the data in Table 8, $\delta V_0/V_0 = 0.17$. The relative standard error of the kinetic energy is 0.34.

The uncertainty in the calculated efficiencies should include the uncertainty in the explosive mass and the unit energy. The relative standard error of the explosive mass per hole is 0.03, though for the seismic energy the total mass of explosive has been used and, for the kinetic energy, the mass and the geometrical parameters used were those from the hole behind the rock that was tracked. In both cases, the error in mass should be lower, though we shall retain the 0.03 value in general.

The unit energy is the result of a calculation. The error depends on the manufacturing tolerances of the explosives compositions; for a variation of ANFO formulation (approximately 94/6% ammonium nitrate/oil, nominal) from 95/5 to 93/7, the relative change in energy calculated is about 0.04. Different calculation methods may add uncertainty to the explosive energy value. Comparing the energy values for ANFO used in this paper with those in [2], the standard relative error is 0.009 for the heat of explosion and 0.06 for the useful work to 100 MPa. The

later value is retained. Combining this with the error in mass, a relative error of 0.07 has been attributed to the explosive energy.

Table 10 shows a summary of the standard errors, the main assumptions and the influential parameters of the energy calculations.

4. Discussion

Table 11 summarizes the fragmentation, kinetic and seismic efficiencies obtained. Values of seismic energy, for each blast, are the average of the averages in the top and floor levels. Considering that the heat of explosion is the

Table 10
Errors, influential parameters and assumptions in the energy calculations

Energy	Relative std. error[a]	Main influential parameters	Main assumptions
Fragmentation	0.09	Fracture specific energy	Cubic or spherical fragments
	0.11	Smaller fragment size considered	Constant specific fracture energy for all sizes
Seismic	0.48	Wave velocities	Spherical wave
	0.49	Particle velocities	Only body waves Radial velocity belongs to a p wave; transverse and vertical velocities to s waves
Kinetic	0.34	Rock ejection velocity	Uniform initial velocity of the rock mass
	0.35		
Explosive	0.07	Composition Calculation method Pressure cut-off for useful work	All energy delivered (heat of explosion)/Some energy discarded (useful work to a certain pressure)

[a]The two values given for the relative standard errors are the upper for the energy and the lower for the efficiency.

Table 11
Summary of energy efficiencies

		Useful work				Heat of explosion			
		Fragment.	Seismic	Kinetic	Total	Fragment.	Seismic	Kinetic	Total
Bench blasts									
15/02		5.0	1.6	8.0	14.6	3.1	1.0	4.9	9.0
29/02		5.2	2.5	16.5	24.1	3.2	1.5	10.3	15.0
37/02		5.7	1.6	6.5	13.8	3.5	1.0	4.0	8.5
43/03		5.9	4.3	8.7	18.9	3.6	2.7	5.4	11.6
45/03		5.8	3.1	5.3	14.1	3.6	1.9	3.3	8.7
50/03		3.1	3.6	9.9	16.6	1.9	2.2	6.1	10.2
54/03		8.8	2.8	5.4	17.0	6.0	1.9	3.7	11.6
58/03		4.5	3.1	14.9	22.5	3.1	2.2	10.2	15.4
420-11		5.7	0.8	26.2	32.7	4.6	0.6	20.7	25.9
440-04		6.9	1.4	4.7	13.0	5.3	1.1	3.7	10.1
	Range	3.1–8.8	0.8–4.3	4.7–26.2	13.0–32.7	1.9–6.0	0.6–2.7	3.3–20.7	8.5–25.9
	Mean	5.7	2.6	10.7	18.8	3.8	1.6	7.2	12.6
Rel. std. error		0.09	0.18	0.19	0.10	0.11	0.16	0.21	0.11
Conf. interval 95%		4.6–6.9	1.7 -3.9	6.9–16.5	15.1–23.3	3.0–4.8	1.2–2.3	4.5–11.4	9.8–16.2
Confined shot			12.9				8.6		
Other works									
[1]						9.7	23.4	3.3	36.4
[2]	Average	0.57	7.0	36.6	44.2	0.33	4.1	21.3	25.7
	Range	0.2–1	2.5–14	13–63	20–69	0.1–0.6	1.5–8	7.5–39	12–40
[3]	Average					0.16	7.5	10.4	18.0
	Range					0.10–0.21	3–12	7.2–12.0	15.4–20.4
[4]							5.3		
[5]							5–9		
[6]							2.7		
[7]							1.8–3.7		
[9]	Average						0.2–5		
	Range						0.1–25		

energy available in the blast, only 8–26% of it has been measured through rock fragmentation, seismic wave and rock movement in bench blasting. The useful work already discards a portion of the total energy, so that the efficiency ranges with respect to it result in somewhat higher values (13–33%). The blasting efficiency (sum of the fragmentation and kinetic) goes from 7 to 25% of the heat of explosion.

The energy components can be described by lognormal distributions (the hypothesis of lognormality cannot be rejected to a 95% confidence level). Using lognormal distributions, relative standard errors of the efficiencies have been calculated as the errors of the logarithmic efficiencies [43]:

$$\delta \ln \eta = \frac{\delta\eta}{\eta} = \sqrt{\frac{s^2}{N} + \frac{s^4}{2(N-1)}}, \tag{31}$$

where N is here the number of production blasts and s^2 the variance of the logarithmic efficiencies. These errors are given in Table 11. They are generally lower than the errors estimated in Section 3.5 (Table 10), as these were obtained from propagation of standard errors of the data in individual blasts while the errors in Table 11, from Eq. (31), are errors of the means.

The standard errors from Eq. (31) have been used to calculate the 95% confidence intervals by a modified Cox method [44]. They are also shown in Table 11.

The value of seismic energy measured for the confined hole was 12.9% (useful work) or 8.6% (heat), much higher than the mean value in the production bench blasts and largely out of the confidence interval. Fig. 6 shows a chart with the energy efficiencies with respect to heat of explosion; the mean values and those corresponding to the blasts of minimum and maximum energies measured are shown. The seismic energy of the confined shot is also shown for comparison.

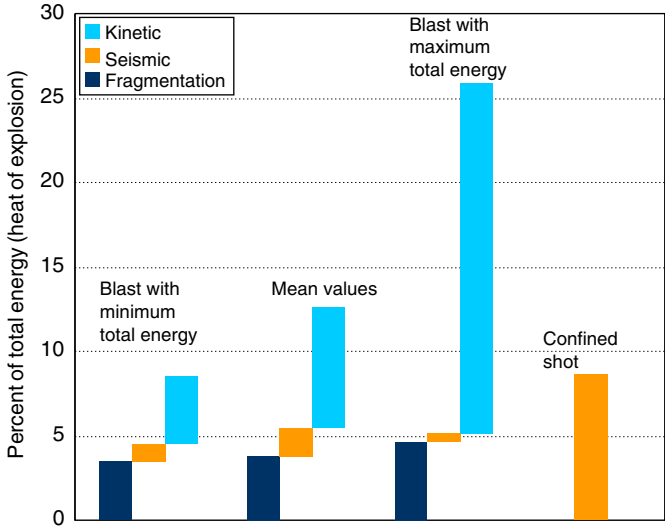

Fig. 6. Energy efficiencies.

The energy not measured (the term E_{NM} in Eq. (1) accounts on average for almost 87% of the heat of explosion or 81% of the useful work.

These results have been compared with data published in the literature, compiled in Table 11. Energy calculations in blasting comprising the three components have been reported in [1–3]; these are discussed first. Other works concerned specifically with seismic energy [4–7,9] are commented on afterwards.

Berta's [1] energy components for bench blasting add up to 36% of the heat of explosion. The kinetic efficiency is in the lower range obtained in the present work. The fragmentation efficiency is higher and the seismic efficiency is one-order of magnitude higher than the results obtained here, much higher than any other studies, and similar to the values reported by Hinzen [9] for extremely confined cutholes in tunnel blasting, which will be discussed hereafter. Berta's energy balance is not based on reported measurements, but on estimations of the various parameters; thus the analysis that can be done on it is limited.

Spathis' [2] energy calculations are based on the data by Sheahan and Beattie [45] for 10 blasts in granite with different explosives, initiation systems and couplings between explosive and rock. The explosive energy was evaluated using the useful work down to 100 MPa (the value Spathis gives for ANFO is 2.3 MJ/kg, similar to the value used in this work, 2.59 MJ/kg). The total energy calculated ranges from about 20% to as high as 69% of the useful work. Spathis' figures have been converted into efficiencies with respect to heat of explosion using the relative strengths reported for the explosives involved [2]. The energy lost below 100 MPa in Spathis' calculations is 42% of the heat of explosion. With reference to heat, the range of total efficiency is from 12% to 40%.

Spathis' fragmentation efficiency is less than our values. This can be attributed to two main aspects of the calculation: (i) the smaller fragment size of the distribution curves was relatively large, 16 mm (for which the cumulative passing ranged from 5% to 2%, not too different from our Eibenstein curves), and (ii) the specific fracture energy used by Spathis (50 J/m^2) was lower than the energies that we have used (172.4 J/m^2 for El Alto's limestone and 294.1 J/m^2 for Eibenstein's amphibolite).

The seismic efficiency reported by Spathis is on average 4.1% of the heat of explosion, more than twice our global mean. Sheahan and Beattie's seismic measurements were all done in the top level, for which the average efficiency in El Alto is 2.5%. One of the reasons for these higher values is the higher compressional wave velocity (5520 m/s) of the granite in which the data by Spathis were obtained, two to four times the wave velocities used in the present work (measured in situ, 2994 and 1705 m/s for p- and s-wave, respectively in El Alto, and 2450 and 1468 m/s in Eibenstein).

Kinetic efficiency has a very ample range, from values similar to ours in the lower limit, to very high values, almost twice our highest value and far from any other

reported elsewhere. Nonetheless, the face velocities used by Spathis ranged from 4.3 to 19.1 m/s, well within our own range.

The energy components from Ouchterlony et al. [3] were obtained in five production blasts in a limestone quarry. The fragmentation efficiency is very low, because the fragment size distributions used for the calculations showed far too little amount of fine material (a fraction of about 0.8% passing at 90 mm, quoted by the authors as a non-credible result from an image analysis, non-calibrated system).

The seismic efficiency (measured in the upper level) is higher by a factor of more than 4 if all our measured values are considered, and by a factor of 3 when compared to our values in the upper level of the limestone quarry (2.5%). The wave speeds in the rock mass used by Ouchterlony et al. (4338 and 5548 m/s) were higher than ours by a factor of two or three so that, though Ouchterlony et al.'s values are higher, the discrepancy is not severe. Some additional reasons that may lead to the higher values of Ouchterlony's seismic measurements are: (i) they were done with accelerometers embedded (anchored to a plate grouted to the rock) at the bottom of a 4 m deep hole in fresh rock; (ii) they were done at closer distance to the blastholes (most of the measurements were at 20–35 m), and (iii) significant existence of water in the rock mass was reported.

The range of Ouchterlony et al.'s kinetic energy fractions (7.2–12%) is within our range of values (3.3–20.7%), though their average is about 40% higher than ours.

In what respects the data by researchers dealing with seismic energy only, [4–7] measure the seismic energy from surface blasts. Howell and Budenstein [4], Fogelson et al. [5] and Nicholls [7] use single, confined blastholes and measurements either on the surface or in holes at varying distances from the shot, from which the seismic energy is obtained by extrapolating the energy function of distance to zero. The distance of the measurements ranged from somewhat less than 1 m to 357 m. The energy rating of explosives is in all of them comparable to the heat of explosion value. The maximum seismic efficiencies are 5.3% [4] (the maximum value is obtained at 12 m from the charge), 9% [5] (zero-intercept of an exponential law of the energy versus a scaled distance $r/W^{1/3}$) and 3.7% [7] (intercept at a scaled distance $r/W^{1/3} = 1$ of a power law). Our 8.6% value for the confined hole appears to be in the upper range of them. Berg and Cook [6] compute the seismic energy from measurements at 6.78–22.0 km from large quarry blasts (550–970 tons of explosive); the zero-intercept energy was 2.7% of the explosive energy.

More recently, Hinzen [9] reports seismic measurements for five blasts made during the excavation of a drift through a gneiss formation, in which three types of explosives were used. The energy description of the explosives is not precise, but a value of 3.21 MJ/kg is reported as "specific energy" for an emulsion, which probably corresponds to the heat of explosion. This value, however, is hardly consistent with the energetic values for the other two explosives involved: 1.39 MJ/kg for an ammonium nitrate gelatine and 2.18 MJ/kg for an ammonium nitrate/TNT/cellulose composition. The seismic efficiency is given for each group of holes in the round; it varied widely, from almost 25% in some of the cut holes (highly confined) to less than 1% for some of the perimeter holes. Considering that the heat of explosion for both the gelatine and the AN/TNT/cellulose should with all probability be in excess of 4 MJ/kg, and that these were the explosives charged in the holes where higher seismic efficiencies were obtained, the actual maximum seismic efficiency was likely to be not more than 8%. For the holes charged with emulsion (rated with a reasonable explosive energy), the average value of the seismic efficiency was about 0.2%; for the holes charged with ammonium nitrate/TNT/cellulose it was about 0.5%, and for the gelatine (rated with a very low energy) it was about 5% when the cut holes were ignored in the analysis. These values (particularly the last one) would have been significantly lower if a higher energy figure would have been assigned to the explosives in question.

The following summary can be drawn from the preceding discussion:

1. *Fragmentation efficiency*: The fines tail of the size distribution curve has obviously a great influence in the resulting value, as fines have a large specific surface and consequently a great amount of the fracture energy is required for their generation. The integral formulation for the area of the smaller size class in the present work includes all this area. As a result, our fragmentation efficiency values are (with the exception of Berta's, who considers a low specific surface area, 80 m^2/m^3, but uses an abnormally high fracture specific surface energy, 1470 J/m^2) comparatively high and should be considered more realistic. This energy could perhaps be somewhat higher if the internal microcracking and the fracture surface roughness were somehow considered. A range from a few units to about 6% of the available energy seems to be spent in rock fragmentation in usual quarry blasting.
2. Seismic efficiency. The fraction of energy conveyed as seismic wave in production blasts may range from as low as less than 1% to nearly 15% of the explosive energy. Though the confined shot's seismic efficiency measured in the present work, 8.6%, is clearly higher (by a factor of more than 5) than the corresponding values for our production blasts, higher values than that have also been reported occasionally in production blasts [3]. Conversely, comparable confined shotholes [4,5,7], and underground cut holes [9], may give seismic efficiencies well below the 8.6% value.
3. Kinetic efficiency. This usually ranges from about 3% to somewhat in excess of 20% of the heat of explosion, though higher values (up to near 40%) have been reported [2].

The average energy lost below 100 MPa for El Alto blasts is 36% of the heat of explosion (the calculation of such value requires the knowledge of the exact composition of the explosives involved, only available for the blasts in El Alto). That energy is conveyed as enthalpy (heat and pressure) of the gases venting to the atmosphere without performing any further work on the rock. Though the 100 MPa cut-off value is to some extent arbitrary [46–49] (and so is the percentage of energy lost), we can still conclude that approximately half of the explosive energy is not made apparent in any measurable physical effect on the rock. Rock blasting is not anything beyond the first principle of Thermodynamics, so what are the mechanisms missing in this balance? There are two of them, very important energy-wise: (i) elastic and plastic work against the rock in the fracture opening that forms the duct network through which the detonation gases flow (the elastic part of it is given back to the medium when the stress is released, or is partially converted to kinetic energy as the fragments detach), and (ii) heat convection from the hot gases to the fracture surfaces, further diffused to the rock mass. Though the detonation process itself is very fast and, due to this, essentially adiabatic, the residence time of the gases within the rock until the movement starts is relatively long; response times (time from the detonation in the hole to the onset of rock movement) can be up to 60 ms, or even longer [50,51], enough for a significant transfer of heat.

The heat transfer is obviously a loss of the process, but the fracture opening is required to break the rock, and it should be put in the useful energy count. It can be that the explosives as work machines are not as inefficient as the low values of measured fragmentation work (accounted as fracture energy only) and kinetic energy spent in rock displacement may, at first instance, indicate. Numerical modeling is required to assess the fracture opening work/heat transfer partition.

5. Conclusions

The basic measurable energy components of the blasting process have been determined from production blasts data. Emphasis has been put on describing in detail the calculations and simplifying assumptions required to derive the energy values from the raw data measured. The following ranges of energetic efficiency (given as the 95% confidence intervals of the means of lognormal distributions) have been obtained for bench production blasts. For each energy component, the first range applies to heat of explosion and the second one to useful work to 100 MPa; values are approximated to the nearest 1%: fracture energy: 3–5%; 5–7%; seismic energy: 1–2%; 2–4%; kinetic energy: 5–11%; 7–16%; total energy measured: 10–16%; 15–23%.

A seismic efficiency for a confined shothole of 9% and 13% with respect to heat of explosion and useful work respectively, has been obtained. This value is higher by a factor of more than five if compared to ordinary production blasts with rock movement. Fracture in the rock surely exists in the confined shot—obviously not measurable—which would put the total energy efficiency figure at a similar level as in the production blasts. In other words, the sum of seismic plus kinetic efficiencies in production blasts is close to the seismic efficiency in the confined shot.

The results of seismic efficiency obtained in the present work, calculated from velocity records measured on the surface, are comparable to other results published from measurements with in-hole embedded gauges, if the effect of the use of in situ p- and s-wave velocities (as opposed to the use of a unique, laboratory P-velocity) is discounted.

The variability of the various energy efficiencies is in some cases quite high, though they are not beyond what is typically encountered in usual blast monitoring. Different blasting features, explosives and rock types, their unavoidable variations within a blast in the field practice and the inaccuracies of the measurements, propagate through the calculations resulting in standard uncertainties for the energies and efficiencies in a given blast up to 50% of the calculated value, with a corresponding wider range of values. This is especially the case for the seismic and kinetic efficiencies and is probably one important reason for the dispersion of the values found by the different researchers. Besides, explosive energies from different sources are sometimes difficult to bring to a common base. With these liabilities, it is possible to set the fractions of explosive energy spent in fragmentation, seismic wave and rock displacement as follows:

1. The fracture energy calculation depends largely on the minimum size of fragments considered. In any case, it may not be expected, in usual quarry blasting, to obtain a fracture energy much in excess of 6% of the total explosive energy.
2. Seismic energy determinations are done generally in an oversimplified manner. A more precise calculation is probably out of reach for a field-blasting situation. Accepting a high-variability consubstantial with all field-blasting measurements, the range of seismic efficiency values reported seems especially wide: values from as low as 0.1% up to, perhaps, 15% of the explosive energy could be expected.
3. The kinetic energy fraction has been found to range, according to our results, from about 3% to 21% of the explosive energy, the higher value corresponding to an overcharged hole. These bounds seem to cover most of the values of kinetic efficiency available though, according to some values in the literature, kinetic efficiency could be up to 40%.

The total energy measured ranges from 8% to about 26% of the explosive energy. The energy spent in useful effects (fragmentation and throw) accounts for 7–25% of the

explosive energy. Some units percent may be in question, but the upper limit is not likely to be much higher in normal blasting practice. It is conceivable, and generally accepted, that explosion gases do not exhaust their energy content in their interaction with the rock, but vent to atmosphere at a relatively high pressure. The amount of energy lost depends on what this pressure is and on the isentropic expansion path, variable from one explosive to another; it has been calculated to be in excess of 30% of the explosive energy for the explosives used in the present work. Adding up this energy to the measured fractions, there remains unaccounted about 40–60% of the energy, in order to balance the energy delivered by the explosive. This energy must have been indeed transferred from the gases to the rock, in the form of rock deformation work and heat transfer.

The energetic analysis provides a good insight of the explosive/rock interaction and a better understanding of the blasting process, encompassing a broad range of scientifically challenging subjects. However, the central issues in rock blasting in the engineering practice (i.e., steer fragmentation towards coarser or finer distributions, reduce vibrations, etc.) comprise a limited fraction of the total explosive energy, with a variance of the same order of their magnitude. An analysis of such variance in relation with blast design parameters and explosive and rock properties is required before energetic arguments may be implemented into engineering design methods for rock blasting. No such analysis has been attempted with the data presented in this work, or with the other (relatively scarce) data existing in the literature; for that analysis to bear statistical significance, the amount of data needed is much larger than what is currently available.

Acknowledgements

The experimental work has been partially funded by the European Union under contract no. G1RD-CT-2000-00438, ''Less Fines Production in Aggregate and Industrial Minerals Industry''. We would like to thank our colleagues in the project for the fruitful research cooperation; especial recognition is due to the technical staff at the quarries of El Alto and Eibenstein for their enthusiastic involvement and valuable assistance in the measurements. Finally, we are indebted to Finn Ouchterlony, of Swebrec at Luleå University of Technology, for many helpful discussions in the preparation of this work and for his scientific advice during the last years.

References

[1] Berta G. L'esplosivo strumento di lavoro. Milan: Italesplosivi; 1990. p. 31–64.
[2] Spathis AT. On the energy efficiency of blasting. In: Proceedings of the sixth international symposium on rock fragmentation by blasting, Johannesburg, 8–12 August. Johannesburg: The South African Institute of Mining and Metallurgy; 1999. p. 81–90.
[3] Ouchterlony F, Nyberg U, Olsson M. The energy balance of production blasts at Norkalk's Klinthagen quarry. In: Holmberg R, editor. Proceedings of the second world conference on explosives and blasting, Prague, 10–12 September. Rotterdam: Balkema; 2003. p. 193–203.
[4] Howell BF, Budenstein D. Energy distribution in explosion-generated seismic pulses. Geophysics 1955;20(1):33–52.
[5] Fogelson DE, Atchinson TC, Duvall WI. Propagation of peak strain and strain energy for explosion-generated strain pulses in rock. In: Proceedings of the third US symposium on rock mechanics, Golden, CO, 20–22 April. Golden: Colorado School of Mines; 1959. p. 271–84.
[6] Berg JW, Cook KL. Energies, magnitudes and amplitudes of seismic waves from quarry blasts at Promontory and Lakeside, Utah. Seismol Soc Bull 1961;51(3):389–400.
[7] Nicholls HR. Coupling explosive energy to rock. Geophysics 1962;27(3):305–16.
[8] Atchinson TC. Fragmentation principles. In: Pfleider EP, editor. Surf Mining. New York: The American Institute of Mining, Metallurgical and Petroleum Engineers; 1968. p. 355–72.
[9] Hinzen KG. Comparison of seismic and explosive energy in five smooth blasting test rounds. Int J Rock Mech Min Sci 1998;35(7):957–67.
[10] Grady DE. Fragmentation under impulsive stress loading. In: Fourney WL, Boade RR, Costin LS, editors. Fragmentation by blasting. Bethel, CT: Society for Experimental Mechanics; 1985. p. 63–72.
[11] Hamdi E, du Mouza J, Fleurisson JA. Evaluation of the part of blasting energy used for rock mass fragmentation. Int J Blast Fragment 2001;5(3):180–93.
[12] Achenbach JD. Wave propagation in elastic solids. Amsterdam: Elsevier; 1975. p. 166.
[13] Rinehart JS. Stress transients in solids. Santa Fe, New Mexico: Hyperdynamics; 1975. p. 41.
[14] Chiappetta RF, Mammele ME. Analytical high-speed photography to evaluate air decks, stemming retention and gas confinement in presplitting, reclamation and gross motion applications. In: Fourney WL, Dick RD, editors. Proceedings of the second international symposium on rock fragmentation by blasting, Keystone, Colorado, 23–26 August. Bethel, CT: Society for Experimental Mechanics; 1987. p. 257–301.
[15] Hamdi E, du Mouza J. A methodology for rock characterization and classification to improve blast results. Int J Rock Mech Min Sci 2005;42:177–94.
[16] Goetz D, Rouabhi A, Tijani M. Mechanical behaviour of rocks. Technical report 35, EU project GRD-2000-25224. Paris: École National Supérieure des Mines; 2002.
[17] Böhm A, Mayerhofer R. Mechanical fragmentation tests. Technical report 10, EU project GRD-2000-25224. Leoben: University of Leoben; 2002.
[18] Sanchidrián JA, Segarra P, López LM. Blasting performance in El Alto quarry (Cementos Portland). Technical report 43. EU project GRD-2000-25224. Madrid: Universidad Politécnica de Madrid; 2003.
[19] Sanchidrián JA, Segarra P, López LM. Blasting performance in Eibenstein (Hengl Bitustein). Technical report 42. EU project GRD-2000-25224. Madrid: Universidad Politécnica de Madrid; 2003.
[20] Bjarnholt G, Holmberg R. Explosive expansion work in underwater detonations. In: Proceedings of the sixth international symposium on detonation, Coronado, California, 24–27 August. Arlington, Virginia: Office of Naval Research, Department of the Navy; 1976. p. 540–50.
[21] Mohanty B. Explosives performance—the underwater test revisited. In: Proceedings Explo'99, Kalgoorlie, 7–11 November. Carton Victoria, Australia: The Australasian Institute of Mining and Metallurgy; 1999. p. 131–7.
[22] Nyberg U, Arvanitidis I, Olsson M, Ouchterlony F. Large size cylinder expansion tests on ANFO and gassed bulk emulsion explosives. In: Holmberg R, editor. Proceedings of the second world conference on explosives and blasting technique, Prague, 10–12 September. Rotterdam: Balkema; 2003. p. 181–91.

[23] Sanchidrián JA, López LM. Calculation of the explosives useful work-comparison with cylinder test data. In: Holmberg R, editor. Proceedings of the second world conference on explosives and blasting technique, Prague, 10–12 September. Rotterdam: Balkema; 2003. p. 357–61.
[24] Sanchidrián JA, López LM. Calculation of the energy of explosives with a partial reaction model. Propell Explos Pyrotechn 2006;31(1):25–32.
[25] Hobbs ML, Baer MR. Nonideal thermoequilibrium calculations using a large product species data base. Report SAND92-0482. Albuquerque, NM: Sandia National Laboratories; 1992.
[26] Hobbs ML, Baer MR. Calibrating the BKW-EOS with a large product species data base and measured C-J properties. In: Proceedings of the tenth international detonation symposium, Boston, MA, July 12–16. Arlington, Virginia: Office of Naval Research; 1993. p. 409–18.
[27] Dap 2 and Danubit 4 data sheets. Bratislava: Istrochem, 2002.
[28] Sanchidrián JA, Segarra P, López LM. A practical procedure for the measurement of fragmentation by blasting by image analysis. Rock Mech Rock Eng 2005; published online.
[29] Kemeny J, Girdner K, Bobo T, Norton B. Improvements for fragmentation measurement by digital imaging: accurate estimation of fines. In: Proceedings of the sixth international symposium on rock fragmentation by blasting, Johannesburg, 8–12 August. Johannesburg: The South African Institute of Mining and Metallurgy; 1999. p. 103–9.
[30] Split-Desktop Software Manual. Tucson, Arizona: Split Engineering LLC, 2001.
[31] Moser P, Cheimanoff N, Ortiz R, Hochholdinger R. Breakage characteristics in rock blasting. In: Holmberg R, editor. Proceedings of the first world conference on explosives and blasting technique, Munich, 6–8 September. Rotterdam: Balkema; 2000. p. 165–70.
[32] Moser P. Less Fines production in aggregate and industrial minerals industry. In: Holmberg R, editor. Proceedings of the second world conference on explosives and blasting technique, Prague, 10–12 September. Rotterdam: Balkema; 2003. p. 335–43.
[33] Schleifer J, Tessier B. Fragmentation assessment using the Fragscan system: quality of a blast. In: Holmberg R, editor. Proceedings of the first world conference on explosives and blasting technique, Munich, 6–8 September. Rotterdam: Balkema; 2000. p. 111–5.
[34] Ouchterlony F. Influence of blasting on the size distribution and properties of muckpile fragments, a state-of-the-art review. MinFo project P2000-10. Luleå, Sweden: Swebrec-Luleå University of Technology; 2003. p. 89–95.
[35] Latham JP, Kemeny J, Maerz N, Noy M, Schleifer J, Tose S. A blind comparison between results of four image analysis systems using a photo-library of piles of sieved fragments. Int J Blast Fragment 2003;7(2):105–32.
[36] Ouchterlony F. The Swebrec function. Linking fragmentation by blasting and crushing. Trans Inst Min Metall A 2005;114:29–44.
[37] Blair DP. Soil-embedded detector mounts for seismic monitoring. Geophysics 1995;60(1):120–33.
[38] ISEE. Blasters' Handbook. Cleveland: International Society of Explosives Engineers; 1998. p. 613,732–4.
[39] Wheeler RM. The importance of proper seismometer coupling. In: Holmberg R, editor. Proceedings of the third world conference on explosives and blasting, Brighton, 13–16 September. Rochester: European Federation of Explosives Engineers; 2005. p. 237–43.
[40] Blair DP, Armstrong LW. The influence of burden on blast vibration. Int J Blast Fragment 2001;5(1-2):108–29.
[41] Segarra P, Sanchidrián JA, López LM, Pascual JA, Ortiz R, Gómez A, et al. Analysis of bench face movement in quarry blasting. In: Holmberg R, editor. Proceedings of the second world conference on explosives and blasting technique, Prague, 10–12 September. Rotterdam: Balkema; 2003. p. 485–95.
[42] Motion Tracker™ 2D program user's manual (Version 5.x). Allentown, Pennsylvania: Blasting Analysis International, 2001. 66pp.
[43] Zhou X- H, Gao S. Confidence intervals for the log-normal mean. Stat Med 1997;16:783–90.
[44] Olsson U. Confidence intervals for the mean of a log-normal distribution. J Stat Educ 2005;13(1).
[45] Sheahan RM, Beattie TA. Effect of explosive type on fines generation in blasting. In: Proceedings of the third international symposium on rock fragmentation by blasting, Brisbane, 26–31 August. Carlton Victoria, Australia: The Australasian Institute of Mining and Metallurgy; 1990. p. 413–5.
[46] Mohanty B. Energy, strength and performance, and their implications in rating commercial explosives. In: Proceedings of the seventh annual conference on explosives and blasting technique, Phoenix, Arizona, 19–23 January. Cleveland, Ohio: International Society of Explosives Engineers; 1981. p. 293–306.
[47] Persson PA, Holmberg R, Lee J. Rock blasting and explosives engineering. Boca Raton, Florida: CRC Press; 1994. p. 87.
[48] Cunningham CVB, Sarracino RS. The standardization of explosives ratings by ideal detonation codes. In: Proceedings of the third international symposium on rock fragmentation by blasting, Brisbane, 26–31 August. Carlton Victoria, Australia: The Australasian Institute of Mining and Metallurgy; 1990. p. 345–51.
[49] Katsabanis PD, Workman L. The effect of available energy on blast design. In: Proceedings of the 14th annual symposium on explosives and blasting research, New Orleans, Louisiana, 8–11 February. Cleveland, OH: International Society of Explosives Engineers; 1998. p. 87–96.
[50] Oñederra I, Esen S. Selection of inter-hole and inter-row timing for surface blasting—an approach based on burden relief analysis. In: Holmberg R, editor. Proceedings of the second world conference on explosives and blasting technique, Prague, 10–12 September. Rotterdam: Balkema; 2003. p. 269–75.
[51] Sanchidrián JA, Segarra P, López LM. On the relation of rock face response time and initial velocity with blasting parameters. In: Holmberg R, editor. Proceedings of the third world conference on explosives and blasting, Brighton, 13–16 September. Rochester: European Federation of Explosives Engineers; 2005. p. 375–89.